Influence of a laser beam radial intensity distribution on Zeeman electromagnetically induced transparency line-shapes in the vacuum Rb cell

2013 J. Phys. B: At. Mol. Opt. Phys. 46 175501

(http://iopscience.iop.org/0953-4075/46/17/175501)

J. Phys. B: At. Mol. Opt. Phys. **46** (2013) 175501 (8pp) doi:10.1088/0953-4075/46/17/175501

Influence of a laser beam radial intensity distribution on Zeeman electromagnetically induced transparency line-shapes in the vacuum Rb cell

S M Ćuk, A J Krmpot, M Radonjić, S N Nikolić and B M Jelenković

Institute of Physics, University of Belgrade, Pregrevica 118, 11080 Belgrade, Serbia

E-mail: krmpot@ipb.ac.rs

Received 15 April 2013, in final form 5 July 2013
Published 5 August 2013
Online at stacks.iop.org/JPhysB/46/175501

Abstract

Experimental and theoretical analyses show the effect of laser beam radial intensity distribution on line-shapes and line-widths of the electromagnetically induced transparency (EIT). We used Gaussian and Π (flat top) laser beam profiles, coupling the D_1 transition of ^{87}Rb atoms in the vacuum cell in the Hanle experimental configuration. We obtained non-Lorentzian EIT line-shapes for a Gaussian laser beam, while line-shapes for a Π laser beam profile are very well approximated with Lorentzian. EIT line-widths, lower for Gaussian than for Π, show nonlinear dependence on laser intensity for both laser beam profiles. EIT amplitudes have similar values and dependence on laser intensity for both laser beams, showing the maximum at around 0.8 mW cm^{-2}. Differences between the EIT line-shapes for the two profiles are mainly due to distinct physical processes governing atomic evolution in the rim of the laser beam, as suggested from the EIT obtained from the various segments of the laser beam cross-section.

(Some figures may appear in colour only in the online journal)

1. Introduction

Electromagnetically induced transparency (EIT) [1–3], an effect causing the narrow coherent resonance in a laser transmission through the atomic vapour media, is essential for subjects like slow light and storage of light [4], lasing without inversion [5], frequency mixing [6], Kerr nonlinearities [7], etc. The importance of EIT has become evident after several recent applications, including the development of atomic frequency standards [8, 9] and magnetometers [10, 11]. Prior to EIT, magneto-optical effects, like the ground-state Hanle effect and nonlinear Faraday effect, were studied and their possible application in extremely low magnetic field measurements was shown [12–15]. EIT resonance line-shape and line-width are of interest for many EIT applications. EIT line-shape in alkali vapours contained in gas cells is altered from the fundamental Lorentzian shape of atomic resonances by several factors. In addition to power broadening, thermal motion of atoms in vacuum cells affects the shape of EIT resonance through a transient evolution of the state of the atoms passing through the laser beam [16–18]. The investigation of the temporal evolution of the optical pumping into a dark state in an atomic beam, with special attention given to the influence of the weak external magnetic field, has been performed in [19]. Studies of EIT dependence on laser beam radius [20], laser intensity [21, 22] and radial profile of the laser intensity [16, 23–26] were performed. Recent experiments have shown effects of different laser modes i.e. a Laguerre–Gaussian laser beam gave narrower EIT than a Gaussian laser beam [27]. In buffer gas cells, filled with a mixture of alkali atoms and inert gas at several Torr, EIT line-shapes are influenced by diffusion of the alkali atoms in and out of a laser beam. Such repeated interaction effectively enables Ramsey-induced narrowing and non-Lorentzian EIT line-shape in media where Doppler

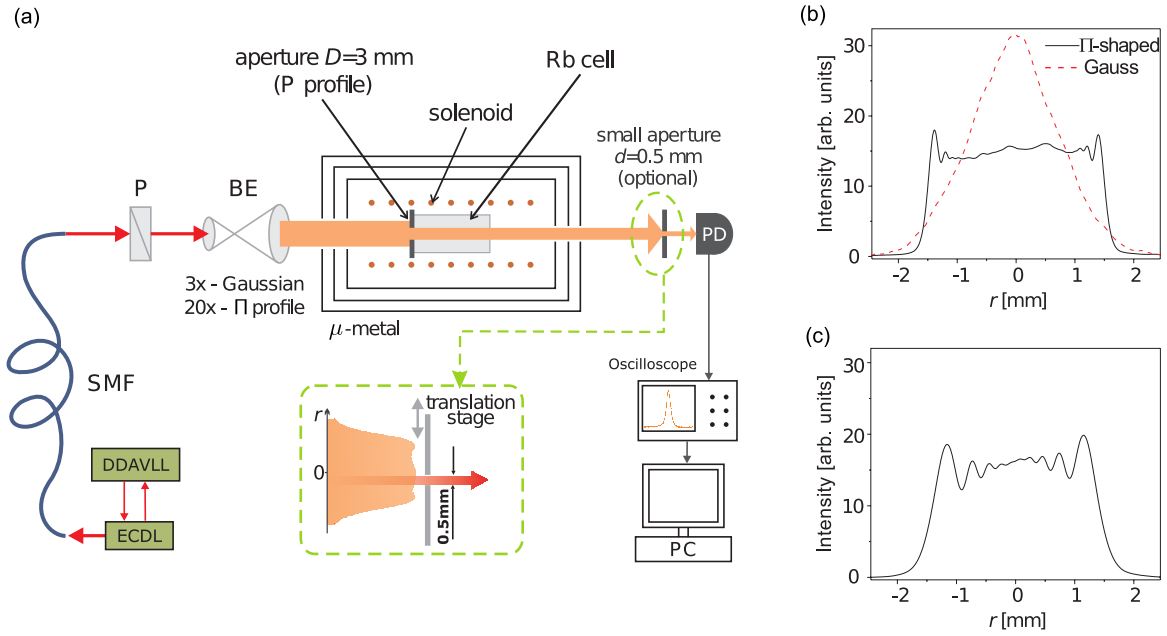

Figure 1. (a) Experimental setup: ECDL—external cavity diode laser; DDAVLL—Doppler-free dichroic atomic vapour laser lock; SMF—single-mode fiber; P—polarizer; BE—beam expander; PD—large area photo diode. For certain measurements the small aperture on the translation stage is placed in the laser beam allowing only a selected part of the laser beam cross-section to reach the detector, while the rest of the laser beam is blocked. Π-shaped beam profiles were recorded by a beam profiler placed at 3 cm (b) and 30 cm (c) from the 3 mm circular aperture. (b) The dashed (red) curve is the profile of the Gaussian laser beam of the same power and diameter as the Π-shaped beam. Note that, in order to have the same overall power of the two laser beams, the peak of the Gaussian beam in the present graph has to have double the value of the flat region of the Π-shaped beam if the diameter of the Gaussian beam is measured at $1/e^2$ of the peak intensity.

broadening is not influential (see [28, 29] and references therein).

Theoretical studies of EIT line-shapes in vacuum cells were mainly carried out assuming a Π (flat top) function for the radial intensity distribution of the laser radiation (see [21] and references therein). Measurements of the EIT line-width as a function of the laser intensity [22], performed with the Gaussian laser beam, show different EIT behaviour with laser intensity than theory [21]— theory predicts wider EIT resonances than experiment, with the discrepancy increasing with the laser intensity. The importance of the laser beam profile on the EIT was indeed demonstrated theoretically for the vacuum [26] and the buffer gas cells [23–25]. Our previous studies have shown that the evolution of the states of the atoms passing through laser beams of different profiles is governed by distinct physical processes [17, 18]. Consequently, line-shapes of EIT resonances obtained from various segments of the laser beam cross-section reflect these differences. It is expected that line-shapes of EIT resonances obtained by detecting whole laser beams of different profiles should also present distinct properties. However, there are no detailed investigations of this kind for vacuum alkali-metal vapour cells. In this work we confirm that the mentioned difference in physical processes significantly affects the overall EIT resonance line-shapes. Besides the results of [17, 18], here we take into account relative amplitudes of EIT resonances from various segments of the laser beam cross-section. The goal of this work is to show how laser intensity affects: (a) differences between the whole beam EIT resonances that are obtained using two laser profiles, (b) contribution of EIT resonances from different parts of the laser beam cross-section to the whole beam EIT and (c) necessity of using a realistic laser beam profile in calculations for proper modelling of experimental results.

The present study is concerned with the radial intensity distribution effects of the laser beam on Zeeman EIT line-shapes in ^{87}Rb contained in a vacuum cell. The study was performed using the Hanle technique. EIT resonances are due to Zeeman coherences developed in the $F_g = 2$ hyperfine level of ^{87}Rb by using resonant laser light that couples the $F_g = 2$ level to the excited hyperfine level $F_e = 1$. We have investigated the dependence of the EIT line-widths and amplitudes on the laser beam profile for a wide range of laser intensities, 0.1–4 mW cm^{-2}. Experimental results are compared with the results of the theoretical model that calculates the density matrix elements by taking into account all of the Rb atomic levels (with Zeeman sublevels) that are resonantly coupled by the laser light.

2. Experiment

The Zeeman EIT experiment employs a single laser whose radiation frequency and polarization are stable and well controlled. Essential for Zeeman EIT measurements is the elimination of laboratory stray magnetic fields, and creation of a variable, homogeneous magnetic field over the entire volume of the Rb cell, directed along the axis of the cell. For the present studies, a careful control of the laser diameter and radial distribution of laser radiation is also necessary. A schematic of the experiment is given in figure 1. We used the extended cavity diode laser whose frequency is stabilized to the $F_g = 2 \rightarrow F_e = 1$ transition of the D_1 line in

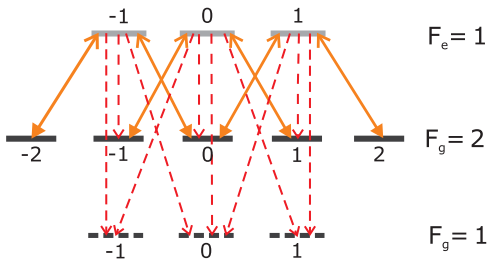

Figure 2. Zeeman sublevels scheme in ^{87}Rb at the D_1 line. The solid lines denote coupling with σ^+ and σ^- components of the linearly polarized laser light. Dashed lines represent spontaneous emission.

^{87}Rb, where F_g and F_e represent the angular momenta of the ground- and excited-state hyperfine levels, respectively. The stabilization scheme is based on the Doppler-free dichroic atomic vapour laser locktechnique [30, 31]. The laser beam is linearly polarized.

The laser beam with Gaussian radial intensity dependence, and 3 mm diameter (measured at $1/e^2$ of the peak intensity), is obtained by the single-mode optical fibre, beam collimator and beam expander. For the Π distribution of the laser beam intensity along its radius, the laser beam behind the fibre is first expanded to about 20 mm, and then the circular diaphragm of 3 mm in diameter is placed over the central part of the laser beam. We used thin foil with a 3 mm hole to obtain the Π profile of laser radiation over the entire length of the Rb cell. The laser beam profile, measured with the commercial beam profilometer, which we consider as the Π radial profile, is given in figures 1(b) and (c), at different distances from the aperture (3 and 30 cm, respectively). In the experiment, this aperture is at the entrance cell window. Laser beam intensity is controlled by the variable neutral density filter. The vacuum Rb vapour cell is 5 cm long and 25 mm in diameter, and is held at room temperature.

The solenoid surrounding the Rb cell produces the magnetic field for the Hanle experiment in the range of $\pm 100\ \mu$T. In order to minimize the stray magnetic fields in the interaction volume, the solenoid and cell are placed inside the triple layered μ-metal. Intensity of the transmitted laser light, as a function of the magnetic field, is detected by the large area photo diode and recorded by the storage oscilloscope. With the small aperture (0.5 mm in diameter) placed in front of the photo diode (with 10 mm in diameter), which we can move along the laser diameter, we were able to obtain EIT resonances only from a small cylindrical segment of the well collimated laser beam.

3. Theoretical model

Zeeman EIT resonances were calculated for the D_1 line transition between hyperfine levels of ^{87}Rb coupled by a linearly polarized laser. The energy level diagram given in figure 2 shows hyperfine levels either coupled to the laser light or populated due to spontaneous emission. The quantization axis is chosen to be parallel to the external magnetic field. The complete magnetic sublevels structure of the transition $F_g = 2 \rightarrow F_e = 1$ is considered in the calculations. The theoretical model is based on time-dependent optical Bloch equations for the density matrix of a moving atom assuming purely radiative relaxation. Equations for density matrix elements related to the ground level $F_g = 1$ are excluded since that level is not coupled by the laser. For additional details about the resulting equations please refer to [18, 26]. It is assumed that after colliding with cell walls, atoms reset into an internal state with equally populated ground magnetic sublevels. Between collisions with cell walls, rubidium atoms interact only with the axially oriented homogeneous magnetic field and spatially dependent laser electric field. Collisions among Rb atoms are negligible due to very low Rb vapour pressure at room temperature, so that an atom moves through the laser beam with constant velocity $\boldsymbol{v} = \boldsymbol{v}_\parallel + \boldsymbol{v}_\perp$, where $\boldsymbol{v}_\parallel$ and $\boldsymbol{v}_\perp$ are longitudinal and transverse velocity components, respectively, with regard to the laser propagation direction. The former affects the longitudinal direction of the atomic trajectory and Doppler shift of the laser frequency seen by a moving atom, while the latter determines the transverse direction of the trajectory and the interaction time. The dependence of the laser intensity on the radial distance r for a Gaussian and Π-shaped profile were modelled using the following equations

$$\begin{aligned} I_{\mathrm{Gauss}}(r) &= 2\bar{I}\exp\left(-2\,r^2/r_0^2\right), \\ I_{\Pi}(r) &= \bar{I}a(1+\mathrm{erf}(p(r_0-r)))^2 \end{aligned} \tag{1}$$

where r_0 is the beam radius, $\bar{I}$ is the beam intensity (total laser power divided by $r_0^2\pi$), a is the normalization constant and p is a positive parameter affecting the steepness of the profile near $r = r_0$. In our calculations we neglect longitudinal changes of the beam profile compared to transverse ones so that only the transverse direction of the trajectory matters. From the reference frame of the moving atom, the electric field varies and the rate of variation depends only on $\boldsymbol{v}_\perp$. Assume that the transverse projection of the atomic trajectory is given by $\boldsymbol{r}_\perp(t) = \boldsymbol{r}_{0\perp} + \boldsymbol{v}_\perp t$, where $\boldsymbol{r}_{0\perp}$ is the perpendicular component of the atom position vector at $t = 0$. The temporal variation of the laser intensity seen by the atom is given by

$$I(t) \equiv I(\boldsymbol{r}_\perp(t)) = I(\boldsymbol{r}_{0\perp} + \boldsymbol{v}_\perp t), \tag{2}$$

representing the spatial laser intensity variation along the trajectory of the atom in the laboratory frame. Additionally, due to the cylindrical symmetry of the beam profile, spatial dependence becomes purely radial dependence.

The observed resonances in EIT experiments are a probabilistic average of the contributions of many individual, mutually non-interacting atoms. Rb atoms traverse the laser beam at different trajectories with different velocities. Maxwell–Boltzmann velocity distribution, diversity of atomic trajectories, the custom cylindrical symmetric radial profile of the laser electric field, effects of the laser propagation along the cell and induced atomic polarization of the Rb vapour are treated similarly as in [18, 26]. The cell temperature was set to room temperature as in the experiment.

4. Results and discussion

In this section we compare EIT resonances obtained with two laser beam profiles in vacuum Rb gas cells. Previous comparisons between the EIT resonances obtained with

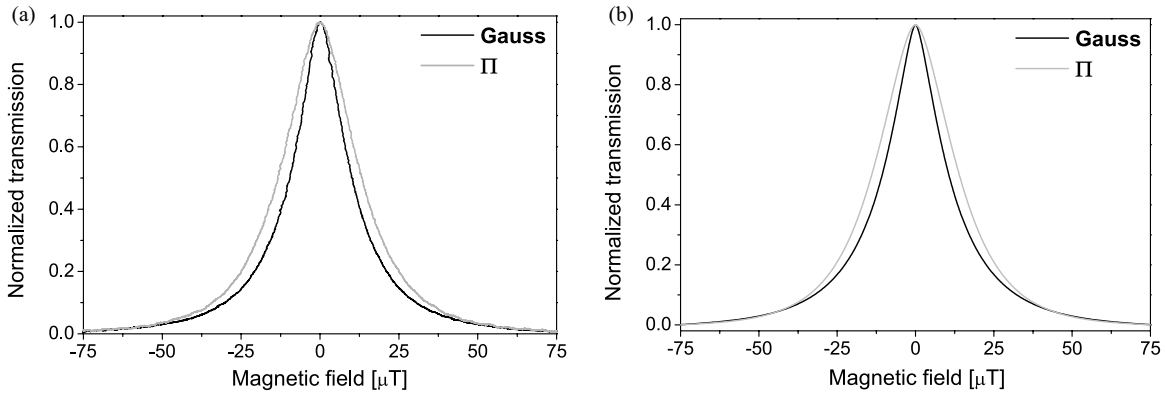

Figure 3. (a) Experimental and (b) theoretical Zeeman EIT resonances obtained by Gaussian and Π laser beam profiles. Laser intensity is 4 mW cm^{-2} and the laser beam diameter is 3 mm for both profiles.

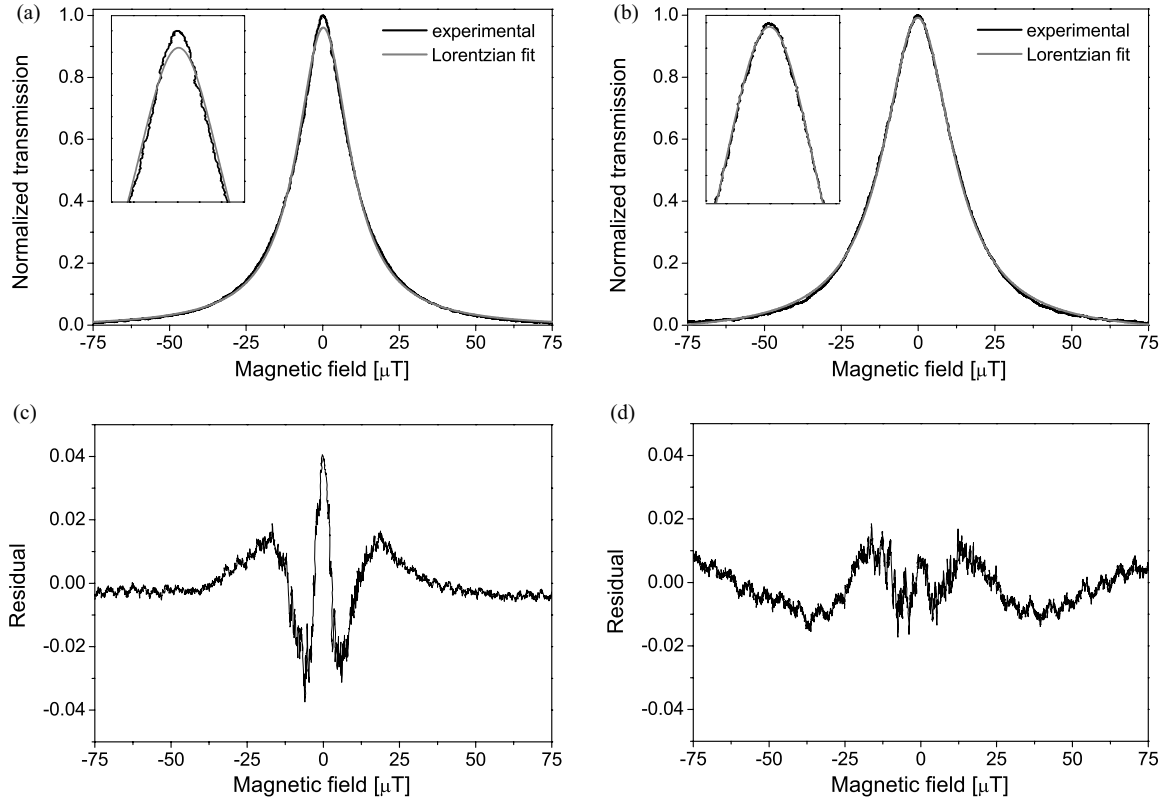

Figure 4. Experimental Zeeman EIT resonances and their Lorentzian fits for the (a) Gaussian and (b) Π laser beam profile. The resonances are obtained under the same conditions like in figure 3(a). Insets show the resonances in the vicinity of their peaks. Residuals, obtained as the difference between the raw data and the corresponding fit, for Gaussian and Π profiles are given in (c) and (d), respectively.

Gaussian and Π laser beam profiles were performed for alkali atoms in buffer gas cells [23–25]. It was calculated, assuming motionless atoms, that EIT line-shapes obtained with a Π laser beam profile are pure Lorentzian. It was also found that the resonances line-shapes are narrower for the Gaussian than for the Π laser beam profile [25]. On the other hand, analysis of the effects of the laser beam shape on EIT in vacuum Rb cells was treated only theoretically [26].

Our EIT resonances were obtained by measuring and calculating the laser transmission as a function of the scanning longitudinal magnetic field, for the Gaussian and the Π laser radial profiles, and for the laser intensity range 0.1–4 mW cm^{-2}. The laser is locked to the $F_g = 2 \rightarrow F_e = 1$ transition of the ^{87}Rb D_1 line. Figure 3 shows measured and calculated resonances for two laser profiles at the laser intensity of 4 mW cm^{-2}. The EIT line-widths and amplitudes, shown and discussed below, were extracted from resonances like these in figure 3, normalized at their maximum values. As seen in figure 3, EIT resonance obtained with the Gaussian laser beam is narrower than the one obtained with the Π laser beam.

If the relaxation of atomic coherences is determined by the radiative decay or by atomic collisions, the line-shapes of the magneto-optical resonances are Lorentzian [16, 23–25, 32]. Experimental resonances and their Lorentzian fits, for the two laser beam profiles, are given in figures 4(a) and (b). It is apparent from these figures, and from residuals between the data and the fits, given in figures 4(c) and (d), that the

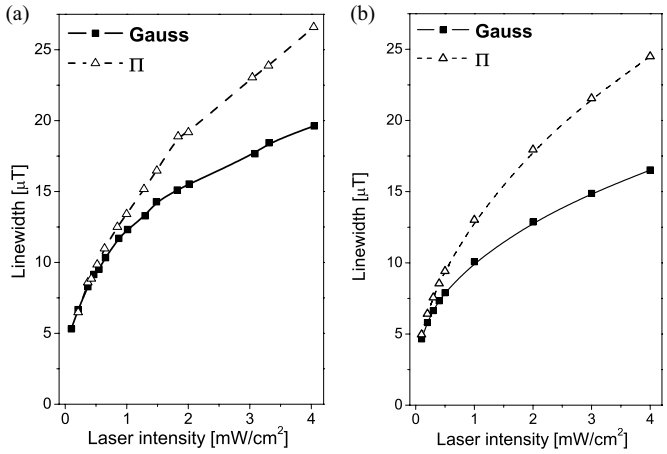

Figure 5. Intensity dependence of (a) experimental and (b) theoretical line-widths of Zeeman EIT resonances for Gaussian and Π laser beam profiles. The beam diameter is 3 mm in both cases. The curves are to guide the eye.

Lorentzian function can better fit the resonance with the Π laser beam profile than with the Gaussian profile. This is particularly the case in the vicinity of a resonance peak, as shown in the insets of figures 4(a) and (b). Corresponding R-square factors, representing the fit goodness, are $R_{\text{Gauss}} = 0.998\,71$ and $R_{\Pi} = 0.999\,341$. These differences between the two profiles remain for all laser intensities.

Figure 4 shows that in an effusive regime of the vacuum cell, the Gaussian laser beam profile gives the EIT line-shape that is narrower in the vicinity of the resonance peak than pure Lorentzian. This is in accordance with the previous results [16] and could be attributed to the time of flight and Ramsey-like narrowing during the free atomic passage through the Gaussian laser beam [17]. In buffer gas cells and diffusive regimes, non-Lorentzian shape (similar to figure 4(a)) is also observed due to the Ramsey effect. However, in buffer gas cells, the Ramsey type narrowing occurs because coherently prepared atoms, after leaving the laser beam and spending time outside of the beam, come back into the laser beam [28]. Line-shapes of the EIT resonances obtained with the Π laser beam profile are Lorentzian. In the case of the Π laser beam profile, laser intensity is constant during the atomic passage through the beam and there is no Ramsey-like narrowing like in the case of the Gaussian beam [17]. In figure 5 we present variations of EIT line-widths with the laser intensity for the two laser beam profiles. As the laser intensity increases the difference between the corresponding EIT line-widths also increases. Theoretical results show very good agreement with the experiment, both qualitatively and quantitatively. For the entire range of laser intensities EIT line-width increases nonlinearly with intensity, but the slope decreases at higher laser powers. This increase in line-width is due to power broadening. For the range of laser intensities as in this work, analytical results, based on the three-level atomic system, predicted square root dependence on laser intensity [21]. What we have observed in the vacuum gas cell is different from line-width dependence on laser intensity in buffer gas cells where the linear dependence of line-width on the laser intensity is reported [25, 33–35].

Without entering into details of the atom–laser interaction for particular laser beam profile, one can give a qualitative argument as to why a Π-shaped laser beam yields broader resonances than the Gaussian laser beam. In vacuum cells Rb atoms traverse a laser beam without collisions and along straight lines. During the transit through the laser beam, the atomic state is influenced by both the laser electric field and the external magnetic field. The laser electric field prepares the atoms into a dark state determined by the laser polarization. In such a state, absorption probability of the laser light is minimal—a manifestation of EIT. The external magnetic field introduces oscillations of the atomic Zeeman ground-state coherences at the corresponding Larmor frequencies, and also degrades the dark state. At low laser intensities, the influence of the magnetic field is more significant, and the dark atomic state degrades more easily. The omnichanging electric field of the Gaussian laser beam decreases the robustness of the dark state with respect to the external magnetic field. If the dark state is more robust, the transmission decreases more slowly with the magnetic field. Therefore, greater robustness of the EIT with respect to the external magnetic field requires a larger magnetic field to halve the peak transmission and hence yields larger EIT line-widths for the Π-shaped beam than for the Gaussian beam.

Differences in robustness of dark atomic states for the two beam profiles are illustrated in figure 6. We present

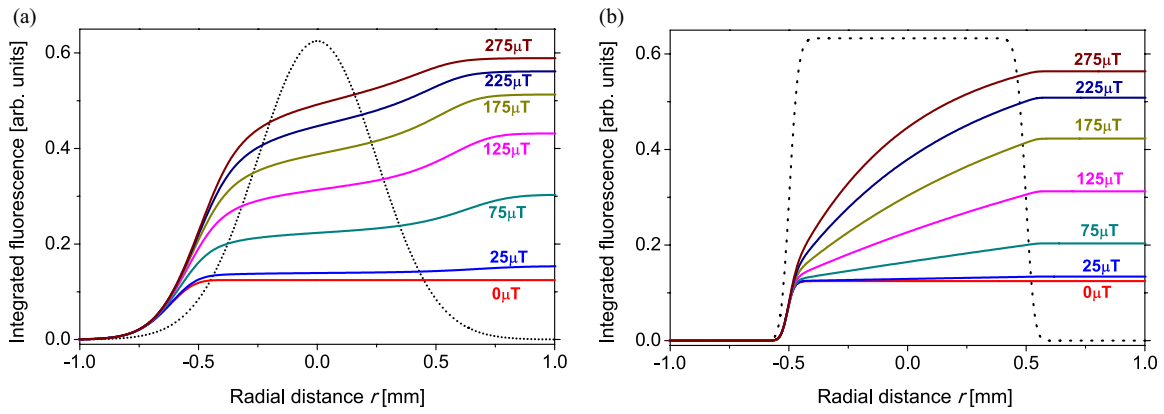

Figure 6. Integrated fluorescence along the atomic trajectory during the atomic passage through (a) Gaussian and (b) Π laser beam at different magnetic fields (given by numbers below each curve). Laser intensity is 4 mW cm^{-2} and radial atomic velocity 180 m s^{-1}.

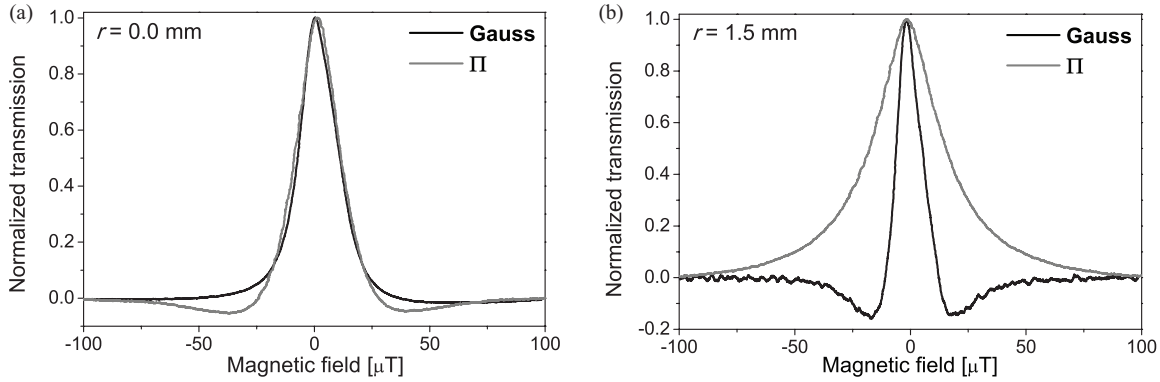

Figure 7. Experimental EIT obtained from only a small circular portion (0.5 mm in diameter) of the laser beam transmitted through the Rb cell when this portion is (a) on the beam axis ($r = 0.0$ mm) and (b) near the beam edge ($r = 1.5$ mm).

fluorescence calculated from the total population of excited Zeeman sublevels of the $F_e = 1$ hyperfine level, integrated along the atomic trajectory that passes through the beam centre, for several values of the external magnetic field. We assume that atom enters the laser beam from the left side with a radial atomic velocity of 180 m s^{-1}, which is the most probable in room temperature Rb vapour. From the curves corresponding to the same magnetic fields, it is apparent that the integrated atomic fluorescence, at the exit of an atom from the laser beam, has increased more for the Gaussian profile than for the Π profile.

In figure 7 we show the EIT obtained by detecting only a portion of the laser beam, defined by (movable) aperture placed in front of the large area photo diode (see section 2 for details). This aperture is centred on the beam axis ($r = 0.0$ mm) for the resonances in figure 7(a), and is near the beam edge ($r = 1.5$ mm) for data in figure 7(b). The EIT resonances obtained near the centre of the laser beam are very similar for two laser beam profiles. A large difference exists between EIT measured with the aperture near the beam edges of these two beam profiles. The Gaussian laser beam produces much narrower Zeeman EIT resonances near its edge than the Π-shaped beam.

Further understanding of what causes different EIT line-widths with two laser beam profiles can be obtained from measurements and calculations of EIT amplitudes at various distances from the beam axis, presented in figures 8(a)–(d). Results are given for two laser beam profiles and for two laser intensities. Amplitudes of EIT resonances are increasing with the distance from the beam axis for both beam profiles, which is more pronounced at higher laser intensities. Amplitudes are the highest in the beam segments that have a high geometrical contribution to the total laser beam cross-section. As seen in figure 7, these are also the segments where the resonances for the Gaussian beam are much narrower than for the Π beam profile. Thus, the results of figures 7 and 8 show that the outer parts of the laser beam cross-section are primarily responsible for the observed differences between EIT line-widths obtained with the two laser beam profiles. Physical mechanisms leading to such differences are explained in detail in [17, 18].

Next, we show the behaviour of the EIT amplitudes obtained with the entire Gaussian and Π laser beams. In

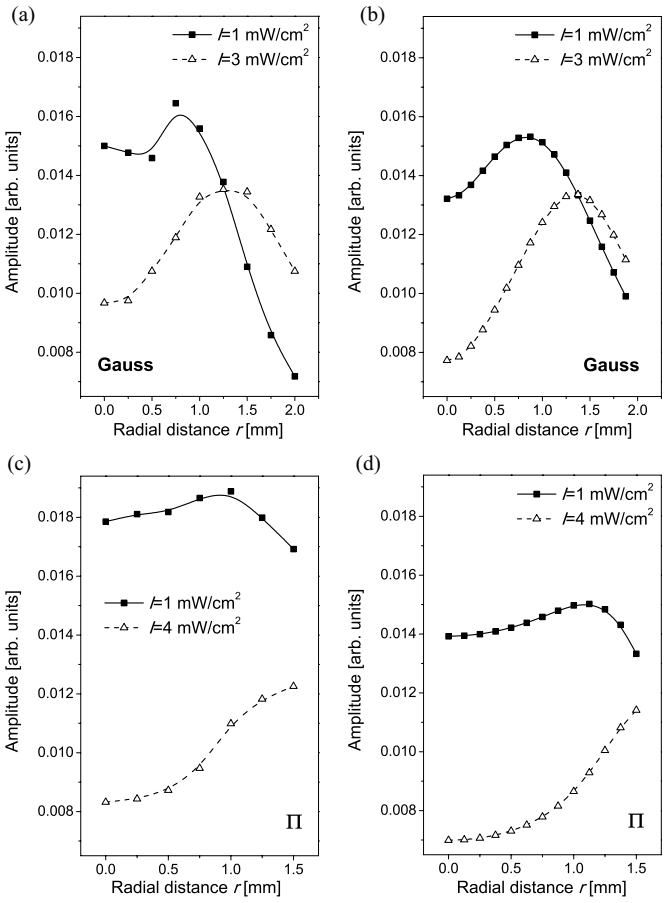

Figure 8. Experimental (a) and (c), and theoretical (b) and (d) amplitudes of the Zeeman EIT resonances obtained at different positions of small aperture along the laser beam radius for the two laser beam profiles.

figure 9 we present measured and calculated EIT amplitudes as a function of the laser intensity. As seen in figure 9, there are no essential differences between EIT amplitudes obtained with the two laser beams. At lower intensities EIT amplitudes show a steep, nearly linear increase with intensity, like in buffer gas cells [36]. The decrease in EIT amplitudes above ∼1 mW cm^{-2} is caused by the increase of the population loss due to optical pumping to the $F_g = 1$ hyperfine level of the Rb ground state, which is not coupled by the laser. Indeed, when the re-pumper

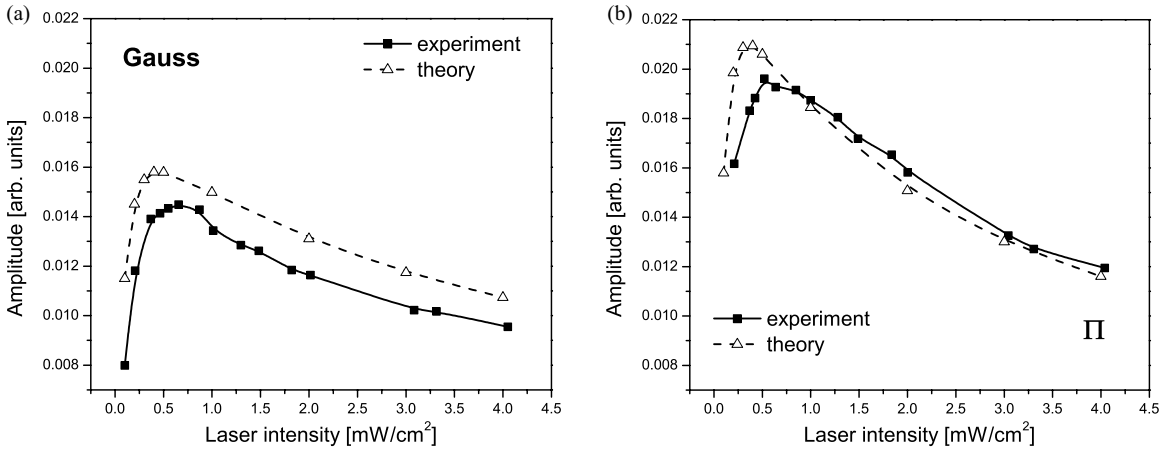

Figure 9. Experimental (solid lines) and theoretical (dashed lines) intensity dependence of Zeeman EIT amplitudes for Gaussian (a) and Π laser beam profile (b). The curves are to guide the eye.

is used to bring the population back to $F_g = 2$ as in [37], the contrast of the amplitudes increases considerably. Figures 9(a) and (b) also show good agreement between experiment and theory.

5. Conclusion

We have demonstrated substantial differences between Zeeman EIT line-shapes and line-widths obtained using two laser radial intensity profiles: Gaussian profile—frequently used in experiments, and Π-shaped laser radial distribution—common in theoretical calculations. Our work is concerned with the effects of these two laser radial profiles on EIT, generated in the Hanle configuration by laser coupling $F_g = 2 \rightarrow F_e = 1$ hyperfine levels in ^{87}Rb atoms in vacuum gas cells. We have shown theoretically and confirmed experimentally the different line-shapes of EIT resonances: those obtained with Π laser beam are very well approximated with Lorentzian, while the Gaussian laser beam profile gives non-Lorentzian Zeeman EIT resonances. EIT resonances are wider for the Π laser beam than for the Gaussian laser beam profile and this difference becomes larger as the laser intensity increases. The study is performed for laser intensities up to 4 mW cm^{-2}. We have shown that major differences in line-widths between two laser profiles are in the regions near the rim of the laser beams. The differences in line-shapes are attributed to different physical processes that Rb atoms undergo during the interaction with the two laser beam profiles. In the wings of the Gaussian laser beam, a Ramsey-like effect can reshape EIT resonances with respect to those near the laser beam centre, as shown in [16, 17]. For the Π profile, optical pumping to the uncoupled ground level dominantly influences the line-shape [18]. The theory demonstrates that the atomic dark state is more sensitive to magnetic field when the atoms are traversing the Gaussian laser beam than when passing through a constant intensity field of the Π laser beam. Larger sensitivity of the atomic dark state to magnetic field variation implies narrower Zeeman EIT line-shapes. The increase of EIT line-widths with the laser intensity is square-root-like for both profiles. Amplitudes of the EIT increase linearly for a laser intensity up to 0.8 mW cm^{-2} for both profiles and decrease at higher intensities due to pumping to the $F_g = 1$ hyperfine level of ^{87}Rb. Observed dependence of line-widths and amplitudes of the EIT with the laser intensity in vacuum gas cells is different from previous results in buffer gas cells.

Acknowledgments

This work was supported by the Ministry of Education and Science of the Republic of Serbia under grant nos 45016 and 171038, and by the Scopes JRP IZ73Z0_127942.

References

[1] Alzetta G, Gozzini A, Moi L and Orriolis G 1976 *Nuovo Cimento* B **36** 5–20
[2] Arimondo E 1996 *Prog. Opt.* **35** 257–354
[3] Fleischhauer M, Imamoğlu A and Marangos J P 2005 *Rev. Mod. Phys.* **77** 633–73
[4] Phillips D F, Fleischhauer A, Mair A, Walsworth R L and Lukin M D 2001 *Phys. Rev. Lett.* **86** 783–6
[5] Scully M O, Zhu S Y and Gavrielides A 1989 *Phys. Rev. Lett.* **62** 2813–6
[6] Harris S E, Field J E and Imamoğlu A 1990 *Phys. Rev. Lett.* **64** 1107–10
[7] Schmidt H and Imamoğlu A 1996 *Opt. Lett.* **21** 1936–8
[8] Knappe S, Shah V, Schwindt P D, Holberg L, Kitching J, Liew L A and Moreland J 2004 *Appl. Phys. Lett.* **85** 1460–2
[9] Affolderbach C, Andreeva C, Cartaleva S, Karaulanov T, Mileti G and Slavov D 2005 *Appl. Phys.* B **80** 841–8
[10] Fleischhauer M, Matsko A B and Scully M O 2000 *Phys. Rev.* A **62** 013808
[11] Belfi J, Bevilacqua G, Biancalana V, Cartaleva S, Dancheva Y and Moi L 2007 *J. Opt. Soc. Am.* B **24** 2357–62
[12] Dupont-Roc J, Haroche S and Cohen-Tannoudji C 1969 *Phys. Lett.* **28** 638–9
[13] Haroche S and Cohen-Tannoudji C 1970 *Phys. Rev. Lett.* **24** 974–8
[14] Weis A, Wurster J and Kanorsky S I 1993 *J. Opt. Soc. Am.* B **10** 716–24
[15] Kanorsky S I, Weis A, Wurster J and Hänsch T W 1993 *Phys. Rev.* A **47** 1220–6
[16] Pfleghaar E, Wurster J, Kanorsky S I and Weis A 1993 *Opt. Commun.* **99** 303–8

[17] Krmpot A J, Ćuk S M, Nikolić S N, Radonjić M, Slavov D G and Jelenković B M 2009 *Opt. Express* **17** 22491–8
[18] Krmpot A J, Radonjić M, Ćuk S M, Nikolić S N, Grujić Z D and Jelenković B M 2011 *Phys. Rev.* A **84** 043844
[19] Korsunsky E A, Maichen W and Windholz L 1997 *Phys. Rev.* A **56** 3908
[20] Li L, Peng X, Liu C, Guo H and Chen X 2004 *J. Phys. B: At. Mol. Opt. Phys.* **37** 1873–8
[21] Javan A, Kocharovskaya O, Lee H and Scully M O 2002 *Phys. Rev.* A **66** 013805
[22] Ye C Y and Zibrov A S 2002 *Phys. Rev.* A **65** 023806
[23] Levi F, Godone A, Vanier J, Micalizio S and Modugno G 2000 *Eur. Phys. J.* D **12** 53–9
[24] Gilles H, Cheron B, Emile O, Bretenaker F and Le Floch A 2001 *Phys. Rev. Lett.* **86** 1175–8
[25] Taĭchenachev A V, Tumaikin A M, Yudin V I, Stahler M, Wynands R, Kitching J and Hollberg L 2004 *Phys. Rev.* A **69** 024501
[26] Radonjić M, Arsenović D, Grujić Z and Jelenković B M 2009 *Phys. Rev.* A **79** 023805
[27] Anupriya J, Ram N and Pattabiraman M 2010 *Phys. Rev.* A **81** 043804
[28] Xiao Y, Novikova I, Phillips D F and Walsworth R L 2008 *Opt. Express* **16** 14128–41
[29] Xiao Y, Novikova I, Phillips D F and Walsworth R L 2006 *Phys. Rev. Lett.* **96** 043601
[30] Petelski T, Fattori M, Lamporesi G, Stuhler J and Tino G M 2003 *Eur. Phys. J.* D **22** 279–83
[31] Wasik G, Gawlik W, Zachorowski J and Zawadzki W 2002 *Appl. Phys.* B **75** 613–9
[32] Castagna N and Weis A 2011 *Phys. Rev.* A **84** 053421
[33] Erhard M and Helm H 2001 *Phys. Rev.* A **63** 043813
[34] Sautenkov V A, Kash M M, Velichansky V L and Welch G R 1999 *Laser Phys.* **9** 889–93 www.maik.ru/full/lasphys/99/4/lasphys4_99p889full.pdf
[35] Figueroa E, Vewinger F, Appel J and Lvovsky A I 2006 *Opt. Lett.* **31** 2625–7
[36] Knappe S, Wynands R, Kitching J, Robinson H G and Hollberg L 2001 *J. Opt. Soc. Am.* B **18** 1545–53
[37] Kazakov G, Mosets I, Rozhdestvensky Yu, Mileti G, Delporte J and Matisov B 2005 *Eur. Phys. J.* D **35** 445–8